FEDERAL COMMUNICATIONS COMMISSION
ENGINEERING DEPARTMENT

DAYTIME SKYWAVE AT BROADCAST FREQUENCIES

An analysis of Data Recorded on 14 Transmission Paths for a Period of Approximately Six Years

The practical and general object of this analysis is to obtain curves representing "10% skywave field intensities" at any distance, in any direction, at any frequency, at any hour of transmitter local time for a station at any latitude.

In order to achieve the most accurate results possible as rapidly as possible this general aim has been limited here somewhat. Only noon, afternoon and evening data have been studied. The empirical curves for 10% fields in the second hour after sunset have been used directly as a point of departure in the deviation of curves representing fields in other hours. This has been done by the simple expedient of applying diurnal curves to the second hour curves. With respect to the first limitation, morning conditions are known to be not quite symmetrical with evening conditions but they have been considered to be nearly enough symmetrical that the difference is of secondary practical importance. The second limitation is more serious but saved a great deal of time without perhaps limiting the immediately useful results very seriously. The chief effec of the direct use of the empirical curves for 10% fields in the second hour after sunset rather than the theoretical formulas for this second hour curve has been to limit the deviation of curves to distances less than approximately 1200 miles.

By "10% skywave field intensity" in a given hour of the day is meant the level exceeded by the hourly median field intensity for 10% of such hours of the year. Such values are devoted in the following by the obvious notation $E_{m\ 10\%}$.

The analysis procedure was of a simple and empirical nature and can be rapidly described:

Figure 1 a, b, c, d, e, f tabulates the $E_{m\ 10\%}$ values by years, a page for each solar hour. SSMP denotes the sunset hour at the path mid-point. This hour was centered on the instant of sunset at the mid-point. SSMP-1 denotes the hour preceeding SSMP and so on. The numbers tabulated are the microvolts per meter recorded (not microvolts per meter per 100 mv/m radiated). The numbers in parenthesis are numbers of data in the annual sample that determined the $E_{m\ 10\%}$ values.

Figure 2 shows a plot of the data for WFAA as recorded in Grand Island, Nebraska. On the SSMP axis, for example, each year's $E_{m\ 10\%}$ value for that hour is plotted as an x with a numeral 9, 0, 1, 2, 3, or 4 beside it to denote the year '39, '40, etc. in which the value was recorded. It will be noted that if a diurnal curve is drawn through each years data, the several curves would cross and re-cross each other. This has been taken to mean that

the data are varying at random--about a diurnal curve typical of all years. The curve shown in the figure is drawn through the median of all years. This curve will be referred to as the composite diurnal curve for G-WFAA, composite referring to its being composite of all years. (Statistically, it enters a new hierarchy of random variation, the random variation from year to year of annual statistics. In this realm it is a median curve.

Similar curves have been drawn for the other data shown in Figure 1. Figure 3 shows a tabulation giving various pertinent data including a tabulation of the ratios of the field values attained in the various hours on the composite diurnal curves for the individual paths to the value attained in SSMP +2. These ratios are denoted by E_{ss+1}/E_{ss+2}, E_{ss}/E_{ss+2}, etc.

Figure 4 shows a plot of these ratios versus frequency for SSMP+1, SSMP, and SSMP-1. It will be noted that the ratios define a trend line rather clearly and that the trend line becomes steeper in regular fashion showing increasing frequency effect in earlier hours. A plot of the SSMP-2 ratios does not define a trend. This has been assumed to mean that most of the data available are at frequencies and distances such that the recorded fields are groundwave fields. Available time did not permit the determination directly from the experimental data of $E_{m10\%}$ values for SSMP +3, nor was it thought at first that they would be of any particular use. In the ultimate application, when diurnal curves extending to time, a little later than SSMP +2 became needed, the composite diurnal curves were extrapolated individually to SSMP+3. The ratio "data" shown in Figure 4 for SSMP +3 were determined by this extrapolation.

A similar plot of the ratios against equivalent vertical incidence frequency shows similarly well defined trends. Means have been sought to determine which is the better representation, but none has yet been found that can determine the question. More will be said on this matter at a latter point in this report.

Figure 5 shows diurnal curves for 0.5, 1.0 and 1.5 mc based upon the ratio trent curves of Figure 4. These curves have been extrapolated by the dashed lines as shown. These extrapolations are made on the basis of the following considerations. The absorption coefficient of skywave during daylight hours may be considered with considerable assurance to be almost symmetrical about the noon-hour and to be simply related--perhaps simply proportional--to the cosine of the sum's zenith angle, so that in the neighborhood of sunrise and sunset the diurnal curve should have, in logarithmic units, a rather long straight section. The dashed straight line extrapolations have been used in the subsequent applications.

By comparison with computed groundwave field intensities, only the A-WCKY, B-WCKY, G-KSTP, and G-WLW and possibly G-WFAA noon data shown in Figure 1 appear to be skywave. On other paths the frequencies and distances are such that skywave first appears between SSMP-2 and SSMP-1. Figure 6 shows a tabulation of groundwave field intensities estimated by use of the Standards' conductivity map, groundwave curves and the so-called db method; together with year to year medians of recorded $E_{m\ 10\%}$ values in the noon hour and in SSMP-2.

In connection with this figure it is pertinent to note that at distances of the order of hundreds of miles, groundwave may be expected to vary from time to time by reason of variation of effective earth conductivity or by reason of variation of the tropospheric component, by a factor of 2 or 3 to 1; meanwhile, tentatively accepted methods of estimating ground wave over earth of varying conductivities differ among themselves by a factor of 2 or 3 to 1 in some cases.

The diurnal curves of Figure 5 were next assumed to be representative of short transmission paths, or first mode paths up to 1000 and 1200 miles. (In this regard however, see comments in conclusion with respect to the effects of the use of equivalent vertical incidence frequency.)

With this assumption the curves of Figure 5 may be applied directly to the E_m 10% curves of Figure 1a of the Standards to determine fields at any distance (in the range of the first skywave mode), in any direction, in any hour of transmitter local time and any latitude.

Figures 7a, b, c show E_m 10% fields to the East and to the West in various hours for a station at 40° latitude and at frequencies of 500, 1000 and 1500 Kc. Figures 8a, b, c, show the corresponding fields to the North and South.

To derive these figures it is necessary to note that the curves of Figure 1a are derived on the basis of data in the second hour after sunset at the Western end of the paths. But this, insofar as reciprocity of transmission east and west may be assumed, may equally well be interpreted as a representation of propagation to the East from a transmitter located at the second hour after sunset. The 40° latitude curves of Figure 1a of the Standards has been drawn in the east direction in Figures 7a, b, c, and labeled TSS+2 (second hour after transmitter sunset). The deviation of the rest of the curve is a matter of the application of an elementary sort of geometry of space and time. For example, in Figure 7a the TSS+2 curve to the East at 800 miles gives an E_m 10% value of 54 uv/m. This datum is pertinent to SSMP+2½, since sunset travels 800 miles per hour at 40° latitude. The 800 mile datum for the TSS+1 curve must fall below 54 uv/m then by the ratio of $E_{SSMP+1\frac{1}{2}}/E_{SSMP+2\frac{1}{2}}$ as shown by the 500 Kc diurnal curve of Figure 5, and so on for earlier hours. The same geometry may obviously be applied to other distances to the East or to the West and to other hours. Thus, Figure 7a is identically equivalent, is merely an alternative representation, of the 40° latitude curve of Figure 1a of the Standards combined with the 500 Kc diurnal curve of Figure 5, and is as accurate as are these two curves in combination. The North-South curves of Figures 8a, b, c, are of course derived by the same geometry.

Figure 9 serves a dual purpose. It shows groundwave curves for land and three ground conductivities 5, 10, and 20 mmhos/m, together with E_m 10% skywave curves to the East and West for various hours at 40° latitude. The figure is drawn for a half-wave antenna radiating 100 uv/m at one mile.

It shows the distances at which, depending on ground conductivity and solar time the observable field (if it were above noise level) would change from groundwave to skywave, and shows for example that at distances greater than about 500 miles the expected E_m 10% field will be skywave.

Figure 9 also shows the limitation to primary service by the distortion zone with the approach of sunset. The ends of the horizontal bars through the intersection points of skywave and groundwave curves mark the distances at which the ratio of groundwave to skywave, or the reciprocal, is 2 to 1. From the inner ends of these bars may be read off the limit of primary service in various hours. These have been read and graphed separately in Figures 10 a, b, c, (Figure 10b and c being based upon computations like that illustrated in Figure 9 but not reproduced here).

Figure 11 is a general figure illustrating relationships between a Class I station of 50 kw and a Class II station of 10 kw located 800 miles to the East at 40° latitude. The frequency and ground conductivities assumed are 1 mc and 10 mmho/m. The skywave curves of both stations are labeled by the time at the Class I station.

Figure 12 shows some of the information that can be read off the curves of Figure 11. It shows for each station the limitation to primary service imposed by the other in various hours near sunset. The vertical axis shows time with respect transmitter sunset as an origin. The lower horizontal axis shows the distance at which primary service is limited while the upper horizontal axis shows the limited field intensity contour. In computing these limitations a ratio of groundwave to undesired skywave of 20/1 has been arbitrarily assumed.

Accuracy and Conclusions.

1. As was pointed out the elaborate detail of Figure 7a, for example, is a result of geometry. The accuracy of Figure 7a depends on the accuracy of (a) the 40° latitude curve from Figure 1a of the Standards, (b) the accuracy of the 500 Kc diurnal curve from Figure 5, (c) the accuracy of the assumption that this diurnal curve is applicable to all short distances.

With respect to (a) it may be said that the curve suffers from several defects, the chief ones being that like its predecessors, it is based upon the assumption of transmitter radiation patterns over a perfectly conducting smooth earth so that deviations of data from the curve may be expected on account of earth conditions; and that it shows no frequency effect so that some deviations of data from the curve may be expected on this account. In this latter regard, however, it may be said that the curve is believed to be rather accurate for middle frequencies at middle latitudes, for high frequencies at high latitudes and low frequencies at low latitudes, but may be a little low for high frequencies at low latitudes and a little high for low frequencies at high latitudes.

At an estimate, deviations of data from this curve by as much as 2/1 should be rare although in very unusual cases where all the parameters that have been "averaged out" combine to produce limitations in the same direction greater deviations are possible.

With respect to (b), it may be noted that the typical maximum deviation of the ratio data from the trend lines of Figure 4 is about 1.4 while the typical maximum deviation of a year's datum from the composite diurnal curve Figure 2 is about 1.5 so that altogether the data from a single year might miss the diurnal curve of Figure 5 by a factor of 2.1.

Thus, in an "unlucky" year on an "un-average" transmission path (unusual ground conductivity and terrain) in a particular hour the deviation from predictions here on these accounts may be as great as 4.2/1. These deviations, however, may go either up or down.

With regard to (c), the data are too sparse and ill-assorted to serve as an adequate test. Some of it suggests that there may be some effect of path-length on the diurnal curve. There is also some theoretical reason to believe that the diurnal curve should be a function not of operating frequency but of equivalent vertical incidence frequency--which would involve path-length. An attempt was made to follow through simultaneously on both bases and the representation of diurnal curves as a function of equivalent vertical incidence frequency together with the geometrical consequencies were carried through far enough to see that although there is a significant difference it is not large. This more elaborate procedure was dropped because time did not permit its completion and because it appeared to be an over-refinement on an otherwise rather elementary type of analysis.

If the only presently available assumption alternative to (c) were true rather than (c), the present representation may be in error by a factor variable in distance, which is about 1.5 at its greatest.

2. The analysis of the data and its representation here is particularly elementary and direct. A sounder analysis would interpret the diurnal curves as diurnal curves for an E-layer reflection coefficient. This would also permit the skywave curves for various hours (as in Figures 7 and 8) to be extended to 2000 miles and beyond. Such an analysis requires, however, the introduction of transmitter radiation patterns in the vertical plane based upon finite earth conductivity and a more elaborate theory of the structure of the skywave curve than that upon which the curves of Figure 1a of the Standards is based. Studies have recently been completed in the FCC Technical Information Division which should make possible a representation of the combined frequency and latitude effects in skywave. The effects are mutually contingent and cannot be expressed as a frequency factor and a latitude factor. This representation should be immediately adaptable to diurnally varying reflection coefficients. The studies are based, essentially, on the representation of skywave set out by Mr. K. A. Norton.

3. Although further refinement of analytical procedure is needed to extend the range of representation of skywave it is believed that the representation in this report is of the right order of magnitude and constitutes a reasonable basis for an evaluation of the practical importance of "daytime" skywave.

FIGURE 1a

HOURLY MEDIAN FIELD INTENSITY LEVEL EXCEEDED ON 10% OF THE NIGHTS IN THE SECOND HOUR AFTER SUNSET.

$E_{m10\%}$(in uv/m)SSMP$\pm$2*

	PATH	1939	1940	1941	1942	1943	1944
1.	**G-WHO	1590	1260	1550	1775	1455	1905
2.	G-KOA	1703	1900	1503	1850	1847	2070
3.	A-WCKY		2750			3470	3300
4.	A-WLW					2257	1956
5.	G-KSTP						2210
6.	G-WCCO	580	630	838	1075	992	1210
7.	B-WLW			989	1237	1338	1735
8.	B-WCKY		1370		1528		1907
9.	G-WLW				519	527	733
10.	G-WFAA		1815	1728	1790	1810	1950
11.	G-WOAI	1065	1040	1027	880	850	
12.	P-CBK				162	156.0	544
13.	G-KFI			155	242	271	232
14.	P-WCCO					21.8	82.8
15.	P-WFAA	50	50	113	97	57.4	140
16.	P-WENR	13	17.7	84	85	91.8	98.5
17.	P-WSB						

* In the years prior to 1942 the sunset hour is centered on the end of the path which darkens last.

** G-Grand Island; A-Atlanta; B-Baltimore; P-Portland

Values for 1943 and 1944 have been raised to give equivalent 50 kw values by correcting for

FIGURE 1b

$E_{m10\%}$(in uv/m)SSMP+1

	PATH	1939	1940	1941	1942	1943	1944
1.	G-WHO	$(86)_{1143}$	$(90)_{1106}$	$(89)_{1300}$	$(117)_{1425}$	$(118)_{1193}$	$(118)_{1515}$
2.	G-KOA	$(89)_{1112}$	$(89)_{1414}$	$(88)_{1291}$	$(171)_{1267}$	$(158)_{1462}$	$(119)_{1645}$
3.	A-WCKY		$(358)_{2634}$			$(277)_{3110}$	$(315)_{2890}$
4.	A-WLW					$(281)_{1562}$	$(301)_{1673}$
5.	G-KSTP					(24) 568	$(122)_{1900}$
6.	G-WCCO	$(85)_{360}$	(90) 644	$(89)_{536}$	$(112)_{759}$	(121) 594	(121)
7.	B-WLW			$(320)_{491}$	$(357)_{819}$	$(338)_{1007}$	$(334)_{1300}$
8.	B-WCKY		$(340)_{1080}$		$(348)_{1190}$		
9.	G-WLW					(313) 291	$(121)_{1045}$
10.	G-WFAA	$(92)_{1018}$	$(91)_{1058}$	$(88)_{1277}$	$(215)_{1406}$	$(308)_{1343}$	$(125)_{1516}$
11.	G-WOAI	(90) 935	(89) 915	818	(341) 655	(310) 727	
12.	P-CBK				(154) 90	(75) 103	(90) 211
13.	G-KFI			$(71)_{81.8}$	$(114)_{153}$	$(117)_{165.8}$	$(118)_{144.5}$
14.	P-WCCO					(72) 8.8	(83) 31.4
15.	P-WFAA	$(58)_{15.7}$	$(85)_{12.8}$	$(79)_{20.9}$	(84) 38.3	(84) 28.7	(90) 69.6
16.	P-WENR	(79) 6.9	(77) 8.1	$(57)_{26.1}$	(36) 13.8	(39) 10.8	(22) 32.4
17.	P-WSB						

Number of data in parentheses.

FIGURE 1c

$E_{m10\%}$(in uv/m)SSMP

	PATH	1939	1940	1941	1942	1943	1944
1.	G-WHO	$(85)_{600}$	$(91)_{320}$	$(91)_{565}$	$(111)_{395}$	$(119)_{465}$	$(116)_{611}$
2.	G-KOA	$(86)_{480}$	$(86)_{525}$	$(86)_{555}$	$(184)_{680}$	$(167)_{452}$	$(119)_{498}$
3.	A-WCKY	$(358)_{1150}$				$(277)_{1310}$	$(315)_{1175}$
4.	A-WLW					$(263)_{450}$	$(319)_{419}$
5.	G-KSTP					$(24)_{532}$	$(121)_{740}$
6.	G-WCCO	$(74)_{182}$	$(88)_{195}$	$(91)_{141}$	$(114)_{222}$	$(122)_{157}$	$(122)_{226}$
7.	B-WLW			$(202)_{67.8}$	$(369)_{193}$	$(330)_{244}$	$(338)_{316}$
8.	B-WCKY		$(333)_{403}$		$(347)_{457}$		
9.	G-WLW					$(302)_{71.6}$	$(122)_{34.7}$
10.	G-WFAA	$(84)_{310}$	$(89)_{303}$	$(87)_{342}$	$(328)_{358}$	$(325)_{422}$	$(108)_{424}$
11.	G-WOAI	329	370	283	$(341)_{210}$	$(310)_{215}$	
12.	P-CBK				$(155)_{9.4}$	$(71)_{30.8}$	$(45)_{75}$
13.	G-KFI				45	50.4	51.6
14.	P-WCCO						
15.	P-WFAA	$(89)_{6}$	$(85)_{1}$	$(77)_{6.5}$	$(76)_{3.5}$	$(78)_{2.3}$	$(94)_{6.95}$
16.	P-WENR						
17.	P-WSB						

Number of data in parentheses.

FIGURE 1d

$E_{m10\%}$(in uv/m)SSMP-1

	PATH	1938	1939	1940	1941	1942	1943	1944
1.	G-WHO	$(55)_{107}$	$(81)_{97}$	$(89)_{75.4}$	$(89)_{112}$	$(118)_{107}$	$(117)_{131}$	$(118)_{168}$
2.	G-KOA	$(50)_{225.0}$	$(81)_{80.0}$	$(84)_{101.0}$	(82) 86.0	(133) 85	$(180)_{128}$	$(120)_{140}$
3.	A-WCKY	$(183)_{154.4}$	$(135)_{240}$	$(349)_{260}$	$(79)_{210}$		$(246)_{337}$	$(342)_{277}$
4.	A-WLW	$(202)_{27.7}$	$(331)_{20.9}$	$(323)_{54.4}$	26.0		$(165)_{70.8}$	(300) 70.2
5.	G-KSTP							$(86)_{235}$
6.	G-WCCO	$(36)_{65.0}$	$(60)_{47}$	$(85)_{52}$	$(75)_{24.3}$	$(98)_{25}$	$(115)_{43.7}$	$(120)_{67.2}$
7.	B-WLW			$(289)_{33}$	$(245)_{13.2}$	$(300)_{36.8}$	$(289)_{21.2}$	$(301)_{74.0}$
8.	B-WCKY			$(305)_{93}$		$(339)_{85.6}$	$(331)_{102}$	$(294)_{147}$
9.	G-WLW					$(326)_{20}$ 11	(215) 9.9	$(122)_{30.2}$
10.	G-WFAA	$(34)_{48}$	$(68)_{46}$	$(84)_{38}$	$(84)_{50.5}$	$(304)_{32}$	$(309)_{39.5}$	$(103)_{56}$
11.	G-WOAI	$(58)_{41}$	$(91)_{53}$	$(90)_{66}$	$(91)_{70}$	(321) 35.5 (27.5	(311) (29.7 (34.7	(123) $_{42.6}$
12.	P-CBK					(155) 4.3	$(55)_{13.5}$	$(27)_{56}$
13.	G-KFI							
14.	P-WCCO							
15.	P-WFAA							
16.	P-WENR							
17.	P-WSB							

Number of data in parentheses.

Signals obscured by noise for paths No. 13-17

FIGURE 1e

$E_{m10\%}$(in uv/m)SSMP-2

	PATH	1938	1939	1940	1941	1942	1943	1944
1.	G-WHO	$(55)_{73}$	$(79)_{47}$	$(84)_{52}$	$(88)_{57}$	$(117)_{67}$	$(119)_{50.4}$	$(115)_{71}$
2.	G-KOA	$(49)_{60.0}$	$(62)_{30}$	$(78)_{29.4}$	$(81)_{31}$	$(133)_{60}$	$(180)_{48.7}$	$(120)_{64.9}$
3.	A-WCKY	$(183)_{26.2}$	$(135)_{88}$	$(336)_{48.5}$	$(77)_{80}$	(66) 2.15	$(247)_{112.5}$	$(343)_{67.4}$
4.	A-WLW	$(195)_{10.6}$	$(315)_{10.5}$	$(290)_{15.0}$	12.0		$(115)_{23.5}$	$(300)_{22.1}$
5.	G-KSTP							$(101)_{21.8}$
6.	G-WCCO	$(37)_{28}$	$(60)_{22.0}$	$(84)_{14.5}$	$(88)_{18.0}$	$(86)_{21.8}$	$(109)_{16.6}$	$(118)_{27.4}$
7.	B-WLW			$(280)_{16}$	$(243)_{14.7}$	$(298)_{16.1}$	$(281)_{16.4}$	$(298)_{19.1}$
8.	B-WCKY			$(239)_{17.0}$		$(339)_{20.0}$	$(331)_{22.4}$	$(281)_{37.3}$
9.	G-WLW					(320) (14.5 (8	(290) 8.2	
10.	G-WFAA	$(33)_{12.9}$	$(69)_{15.2}$	$(83)_{12.0}$	$(79)_{15.0}$	(305) 16.7	$(244)_{11.3}$	$(111)_{21.4}$
11.	G-WOAI	(58) 4.1	(91) 5	(90) 3.0	(78) 3.5	(321) (11.6 (3.7	(311) (11.2 (3.4	(123) (15.7 (9.7
12.	P-CBK					$(157)_{3.3}$	$(64)_{6.8}$	$(22)_{25.2}$
13.	G-KFI							
14.	P-WCCO							
15.	P-WFAA							
16.	P-WENR							
17.	P-WSB							

Number of data in parentheses

FIGURE 1f

$E_{m10\%}$(in uv/m)NOON

	PATH	1938	1939	1940	1941	1942	1943	1944
1.	G-WHO	$(55)_{78}$	$(78)_{43.5}$	$(83)_{50}$	$(90)_{57}$	$(101)_{52}$	$(114)_{47.5}$	$(114)_{63.8}$
2.	G-KOA	$(55)_{56}$	$(88)_{28.0}$	$(80)_{29.5}$	$(90)_{31.0}$	$(135)_{49.5}$	$(178)_{42}$	$(118)_{57}$
3.	A-WCKY	$(183)_{2.23}$	$(135)_{10.5}$	$(344)_{5.5}$	$(81)_{9.5}$	$(26)_{2.95}$	$(245)_{13.2}$	$(343)_{14.7}$
4.	A-WLW	$(199)_{11.2}$	$(327)_{7.9}$	$(308)_{16.8}$	$(332)_{11.0}$		$(142)_{17.8}$	$(300)_{14.9}$
5.	G-KSTP							$(105)_{8.7}$
6.	G-WCCO	$(55)_{23.0}$	$(70)_{14.6}$	$(85)_{15.5}$	$(89)_{16.2}$	$(100)_{15.2}$	$(119)_{14.8}$	$(118)_{23.5}$
7.	B -WLW			$(298)_{14.5}$	$(234)_{13.6}$	$(304)_{13.8}$		
8.	B-WCKY			$(201)_{4.2}$		$(335)_{6.52}$	$(335)_{5.25}$	$(277)_{7.88}$
9.	G-WLW						$(262)_{6.7}$	
10.	G-WFAA	$(46)_{13.7}$	$(68)_{9.6}$	$(79)_{9.8}$	$(86)_{10}$	$(305)_{9.4}$	$(318)_{6.9}$	$(112)_{8.8}$
11.	G-WOAI							
12.	P-CBK							
13.	G-KFI							
14.	P-WCCO							
15.	P-WFAA							
16.	P-WENR							
17.	P-WSB							

Number of data in parentheses
Signals obscured by noise for paths No. 11-17

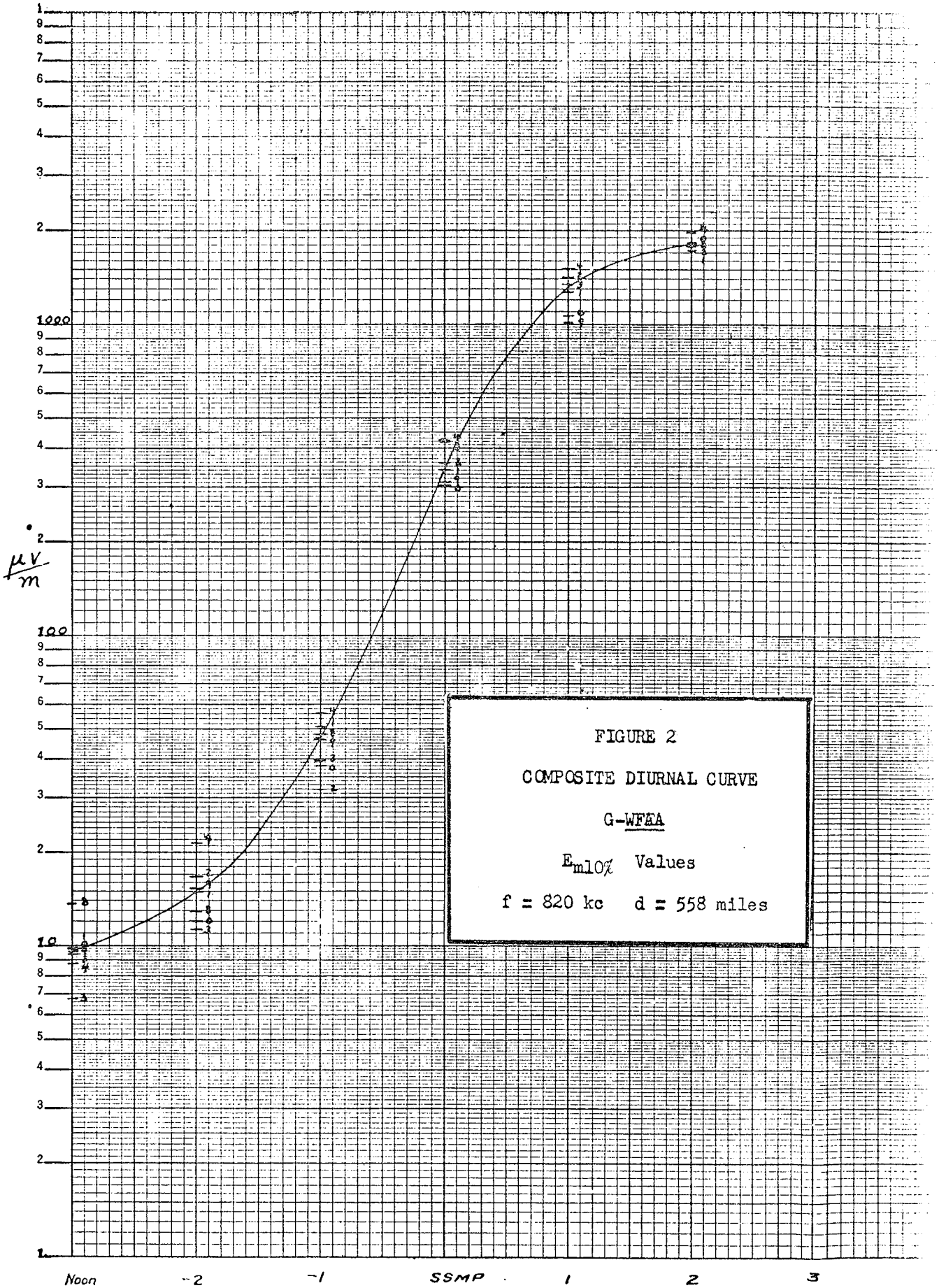

FIGURE 2

COMPOSITE DIURNAL CURVE

G-WFAA

$E_{m10\%}$ Values

f = 820 kc d = 558 miles

TABLE OF TRANSMISSION PATHS STUDIED

Letters A, B, G, P are for receiving stations at Atlanta, Ga., Baltimore, Md., Grand Island, Neb., and Portland Oregon. $E(\phi,0)$ is the radiation at the bearing and pertinent angle. Field ratios are those occurring on the diurnal curves composite of all years.

D. Mi.	Path	F Kc	θ M.P.Lat.	$E(\phi,0)$	$\frac{Ess\,\phi 3}{Ess\,\phi 2}$	$\frac{Ess\,\phi 1}{Ess\,\phi 2}$	$\frac{Ess}{Ess\,\phi 2}$	$\frac{Ess\text{-}1}{Ess\,\phi 2}$	$\frac{Ess\text{-}2}{Ess\,\phi 2}$	$\frac{Enoon}{Ess\,\phi 2}$
268	G-WHO	1040	41.3	915	1.0	.83	.28	.066	.036	.034
343	G-KOA	850	40.4	1820*	1.06	.73	.25	.050	.021	.02
354	A-WCKY	1530	36.5	1270**	1.0	.91	.38	.100	.021	.0035
374	A-WLW	700	36.7	1323	1.085	.76	.21	.034	.011	.0078
387	G-KSTP	1500	43.0	1724	1.0	.84	.34	.071	.010	.0039
390	G-WCCO	830	43.0	1394	1.105	.67	.19	.049	.022	.018
413	B-WLW	700	39.4	1419	1.16	.61	.15	.023	.011	
430	B-WCKY	1530	39.2	1410	1.1	.76	.29	.067	.012	.0044
558	G-WFAA	820	36.9	1593	1.11	.70	.20	.026	.0084	.0056
752	G-WLW	700	40.3	1805		.62	.083	.027	.014	.009
783	G-WOAI	1200	35.2	1642	1.02	.80	.29	.045 est.	est. .0051	
1176	G-KFI	640	38.1	1550	1.16	.63	.20	.018		
1438	P-WCCO	830	46.2	1768	2.4	est. .10	est. .074			
1607	P-WFAA	820	39.9	1768	1.9	.35	est. .038			
1731	P-WENR	890	44.7	1731	2.03	.3				

* For 1940

** For 1943

Figure 3

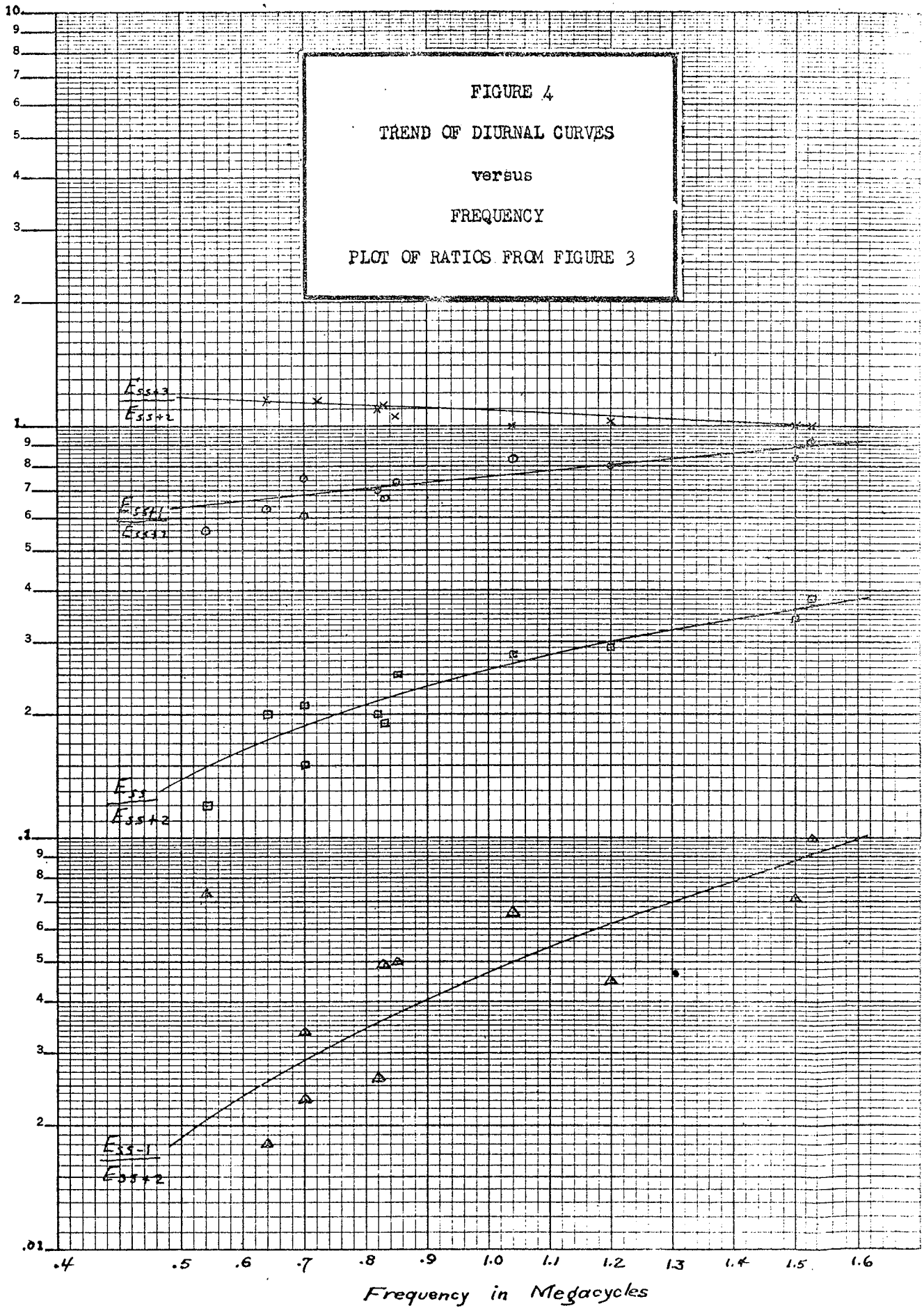
FIGURE 4
TREND OF DIURNAL CURVES
versus
FREQUENCY
PLOT OF RATIOS FROM FIGURE 3
$\frac{E_{ss+3}}{E_{ss+2}}$
$\frac{E_{ss+1}}{E_{ss+2}}$
$\frac{E_{ss}}{E_{ss+2}}$
$\frac{E_{ss-1}}{E_{ss+2}}$
10
9
8
7
6
5
4
3
2
1.
.9
.8
.7
.6
.5
.4
.3
.2
.1
.09
.08
.07
.06
.05
.04
.03
.02
.01
.4
.5
.6
.7
.8
.9
1.0
1.1
1.2
1.3
1.4
1.5
1.6
Frequency in Megacycles

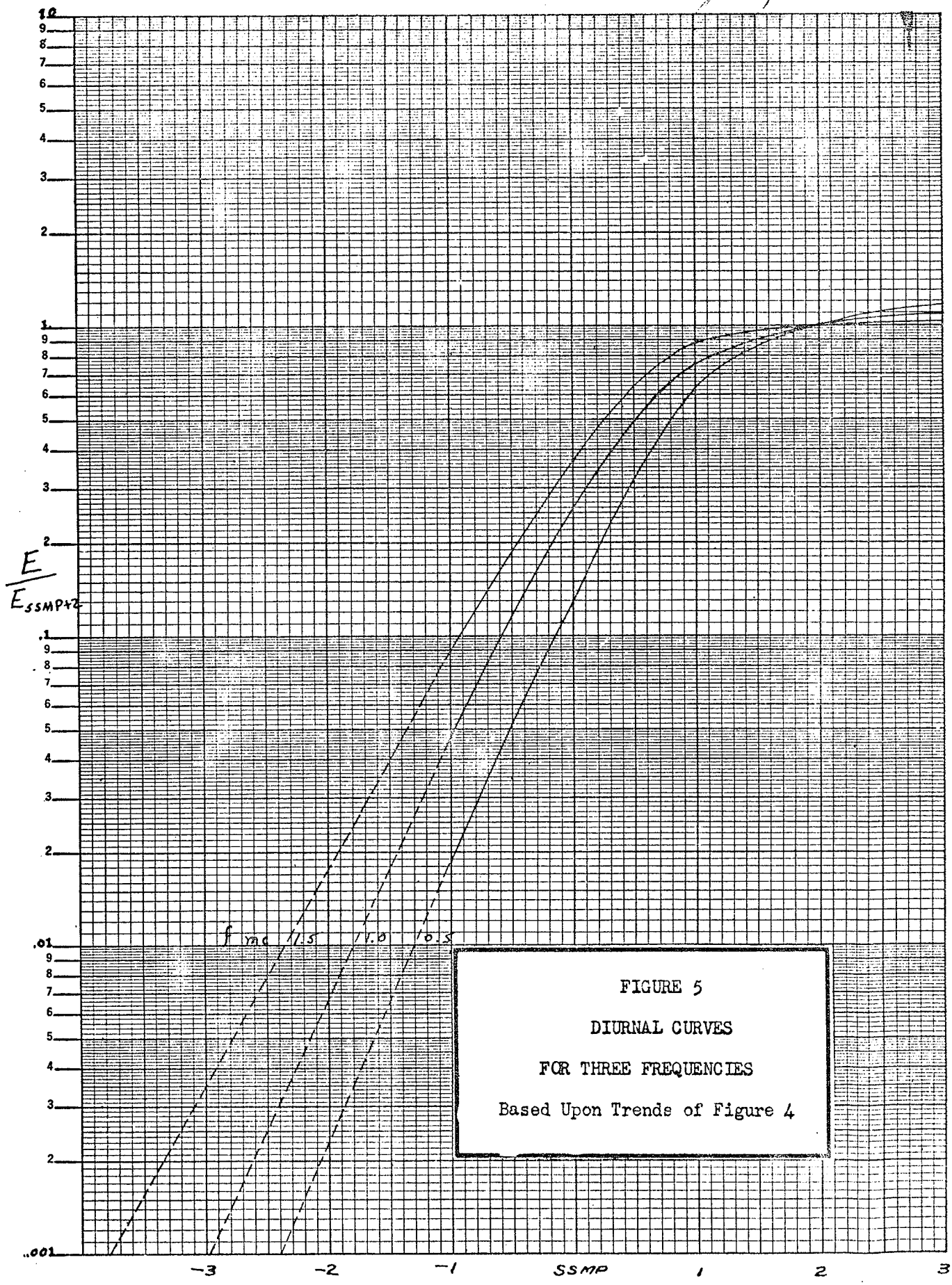

FIGURE 5

DIURNAL CURVES

FOR THREE FREQUENCIES

Based Upon Trends of Figure 4

COMPARISON OF CALCULATED GROUND WAVE FIELD INTENSITIES WITH EXPERIMENTAL LEVELS EXCEEDED 10% OF THE TIME FOR NOON AND SS-2.

	Path	Freq Kc.	Distance Miles	Eff.Field mv/m	Conductivities Miles	Conductivities σ	Field Intensity G.W.Curves uv/m	Medians of 10% Yearly Fields in uv Noon	Medians of 10% Yearly Fields in uv Two Hours Before
1.	A-WLW	700	374	1910	60 40 110 164	10 6 3 2	35.	13.3	13.5
2.	B-WLW	700	413	1910	90 40 60 50 173	10 6 5 3 2	15.	13.8	16.1
3.	G-WLW	700	752	1910	120 40 330 262	10 8 15 20	0. 0.2	6.7	8.2
4.	G-WFAA	820	558	1768	280 160 118	20 15 20	4.8	9.7	15.0
5.	G-WCCO	830	390	1768	80 120 187	8 15 20	15.	15.5	21.8
6.	G-KOA	850	343	1414	120 223	15 20	56.	42.	48.7
7.	G-WHO	1040	268	1626	50 218	15 20	74.	52.	57.
8.	G-KSTP	1500	387	2060	80 120 187	8 15 20	1.2	8.7	21.8
9.	A-WCKY	1530	354	1900	60 40 110 144	10 6 3 2	1.5	9.5	67.4
10.	B-WCKY	1530	430	1900	90 40 60 50 190	10 6 5 3 2	0.4	5.88	21.2

FIGURE 6

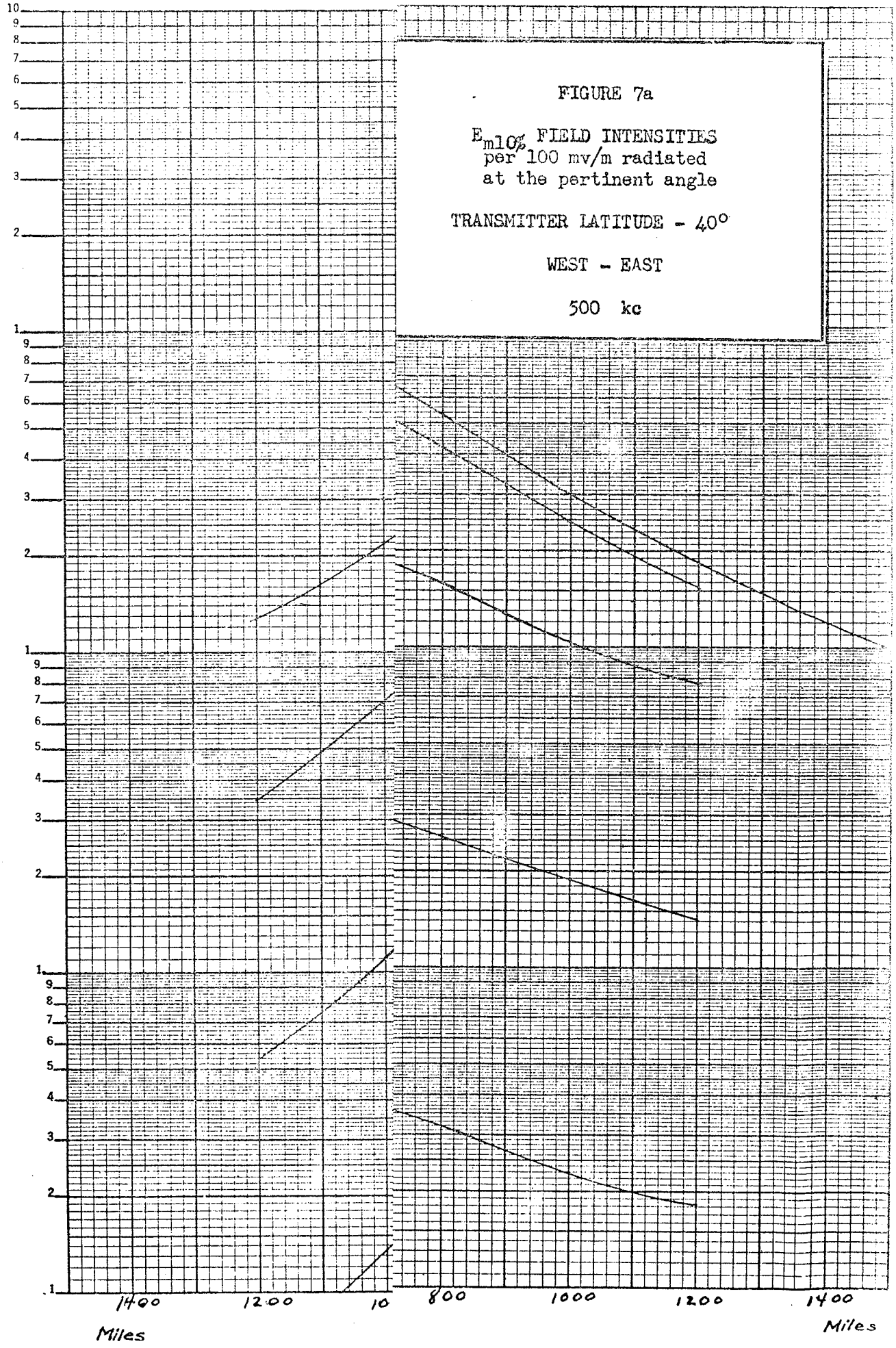
FIGURE 7a
$E_{m10\%}$ FIELD INTENSITIES
per 100 mv/m radiated
at the pertinent angle
TRANSMITTER LATITUDE - 40°
WEST - EAST
500 kc
10
9
8
7
6
5
4
3
2
1
1400
1200
1000
800
Miles

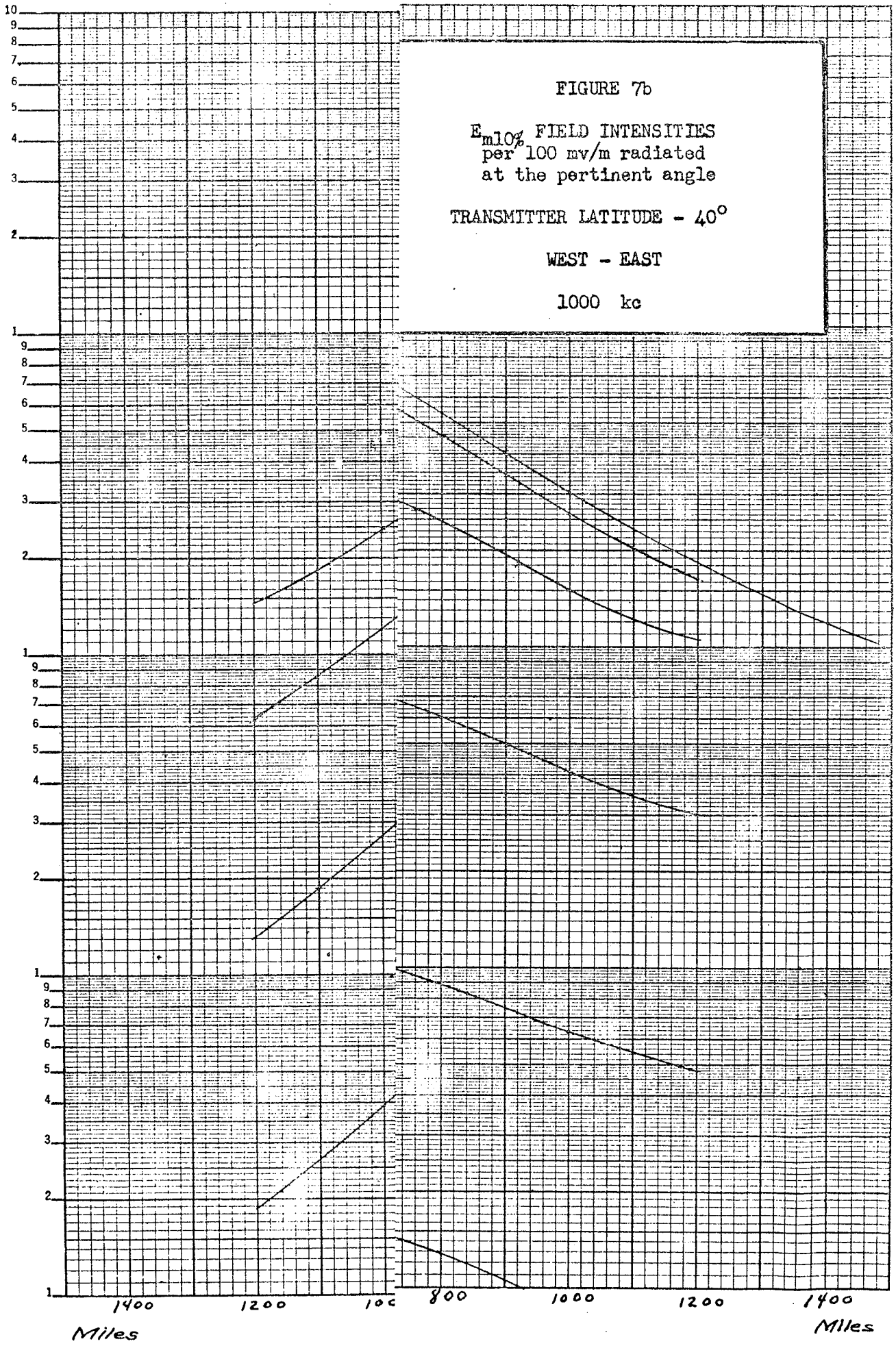
FIGURE 7b
$E_{m10\%}$ FIELD INTENSITIES
per 100 mv/m radiated
at the pertinent angle
TRANSMITTER LATITUDE - 40°
WEST - EAST
1000 kc
10
9
8
7
6
5
4
3
2
1
1400
1200
Miles
800
1000
1200
1400
Miles

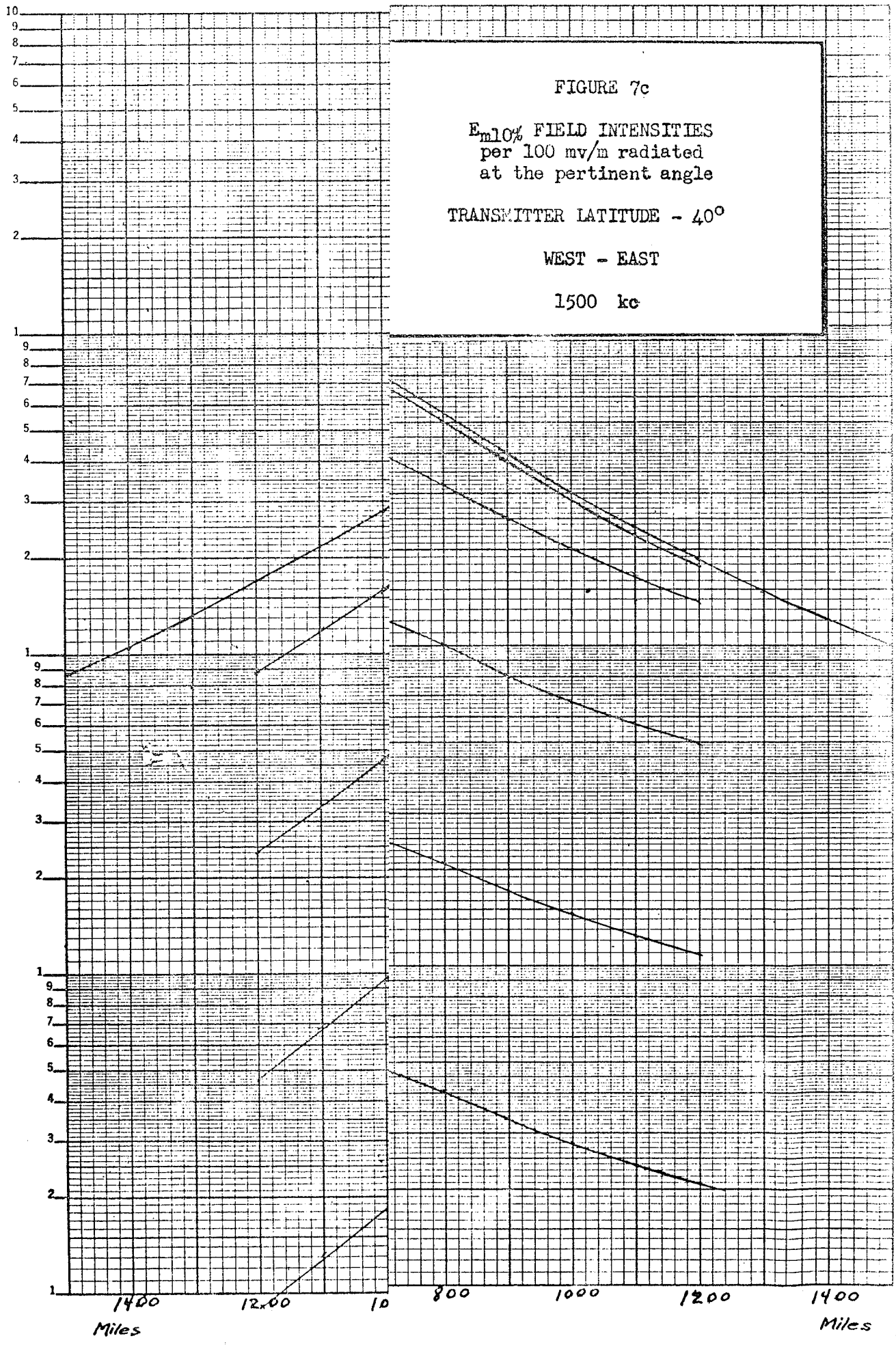
FIGURE 7c
$E_{m10\%}$ FIELD INTENSITIES
per 100 mv/m radiated
at the pertinent angle
TRANSMITTER LATITUDE - 40°
WEST - EAST
1500 kc
10
9
8
7
6
5
4
3
2
1
1400
1200
10
800
1000
1200
1400
Miles
Miles

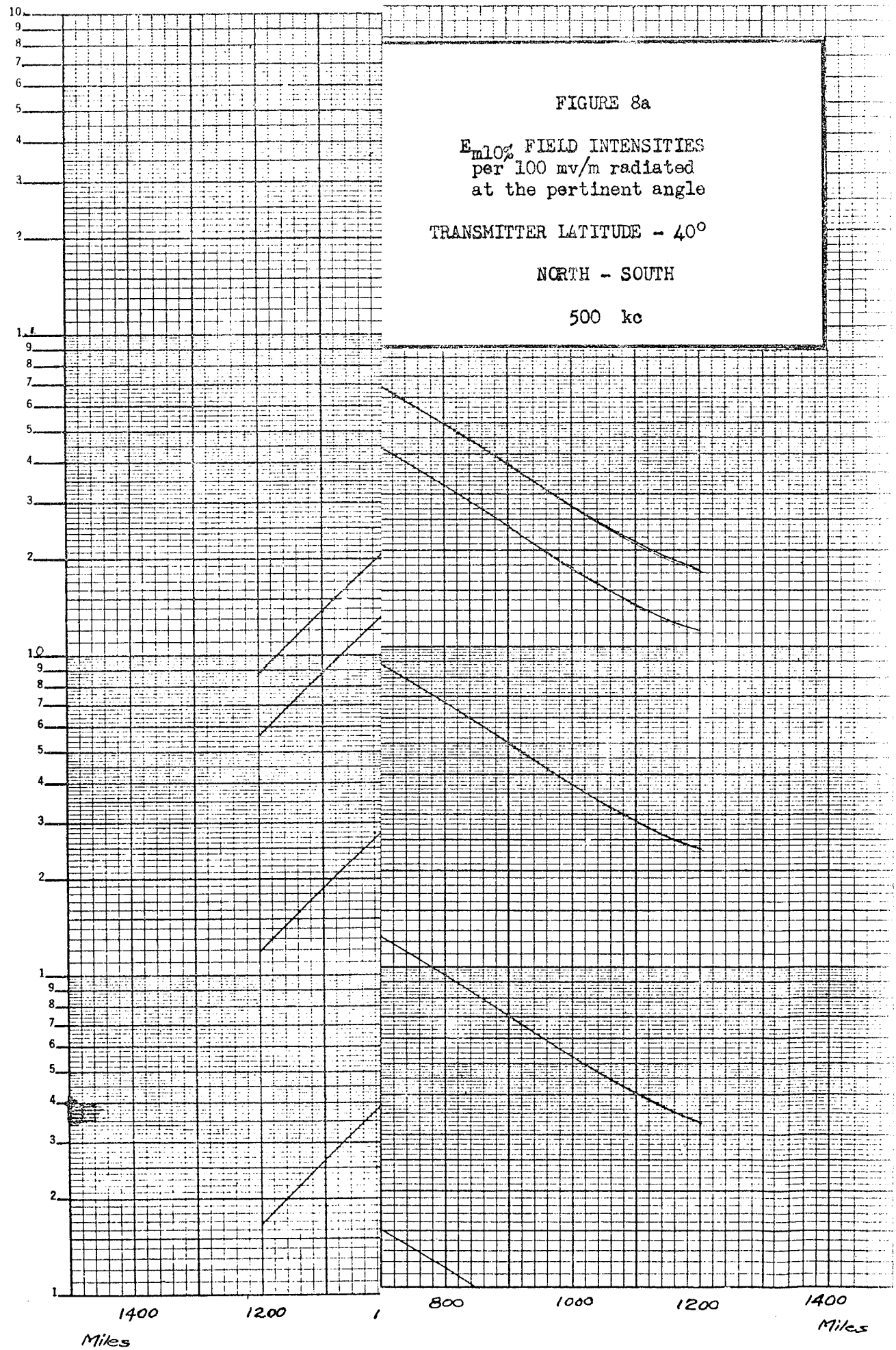
FIGURE 8a
$E_{m10\%}$ FIELD INTENSITIES
per 100 mv/m radiated
at the pertinent angle
TRANSMITTER LATITUDE - 40°
NORTH - SOUTH
500 kc
10
9
8
7
6
5
4
3
2
1
1400
1200
800
1000
1200
1400
Miles
Miles

FIGURE 8b

$E_{m10\%}$ FIELD INTENSITIES
per 100 mv/m radiated
at the pertinent angle

TRANSMITTER LATITUDE - 40°

NORTH - SOUTH

1000 kc

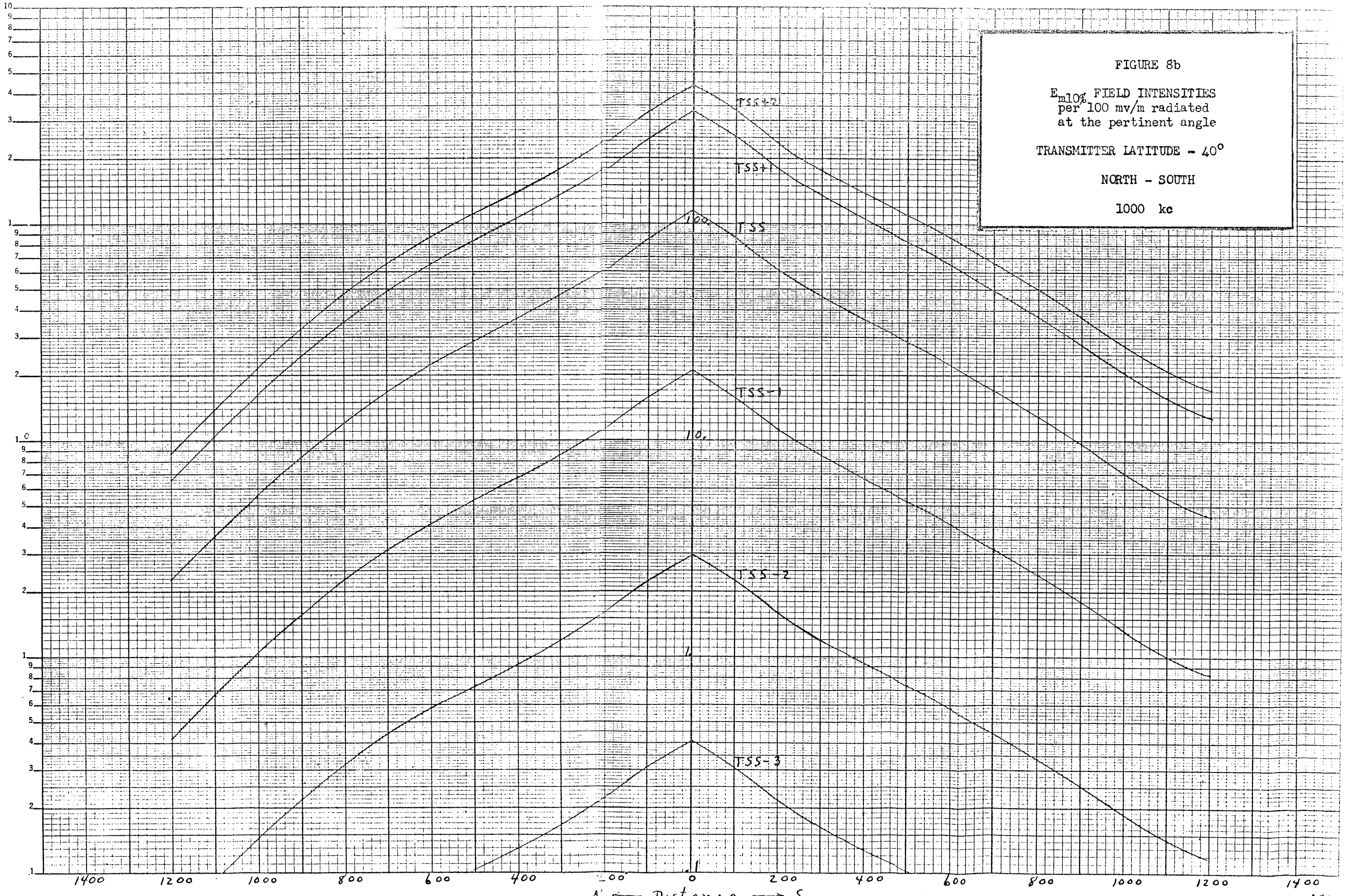

FIGURE 8c

$E_{m10\%}$ FIELD INTENSITIES
per 100 mv/m radiated.
at the pertinent angle

TRANSMITTER LATITUDE - 40°

NORTH - SOUTH

1500 kc

TSS-2

TSS-1

TSS

100 μV/m

TSS-1

TSS-2

TSS-3

10

1

0.1

10
9
8
7
6
5
4
3
2
1
9
8
7
6
5
4
3
2
1
9
8
7
6
5
4
3
2
.1

1400 1200 1000 800 600 400 200 0 200 400 600 800 1000 1200 1400

Miles

North ← Distance → South

Miles

HALF WAVE ANTENNA
HORIZONTAL RADIATION 100 mv/m/M
LATITUDE 40°
σ=10 mmho/m
1000 kc.

FIGURE 9

ILLUSTRATION OF TRANSITION OF FIELD INTENSITIES

FROM

GROUNDWAVE TO SKYWAVE

FOR

VARIOUS HOURS AND VARIOUS CONDUCTIVITIES

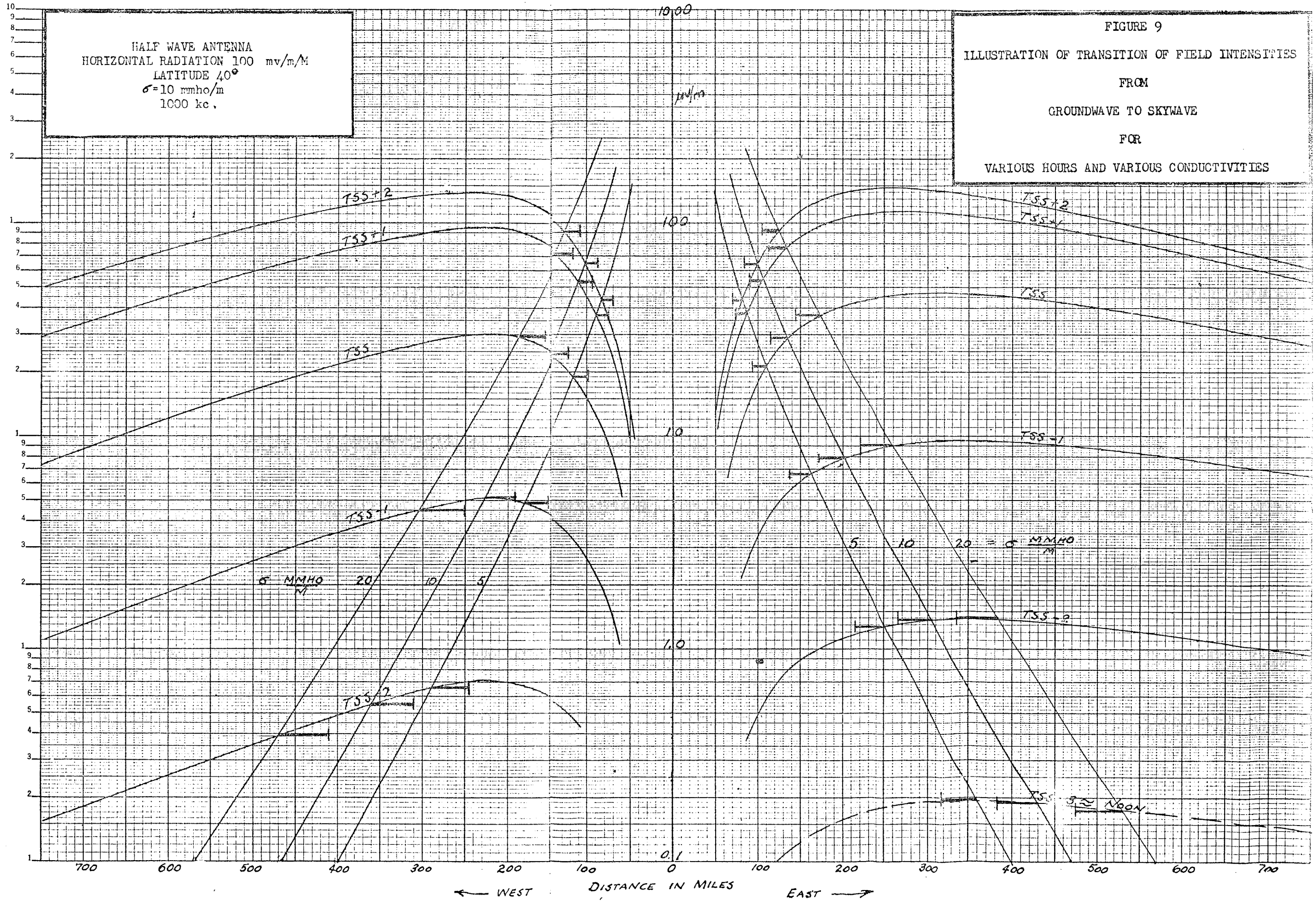

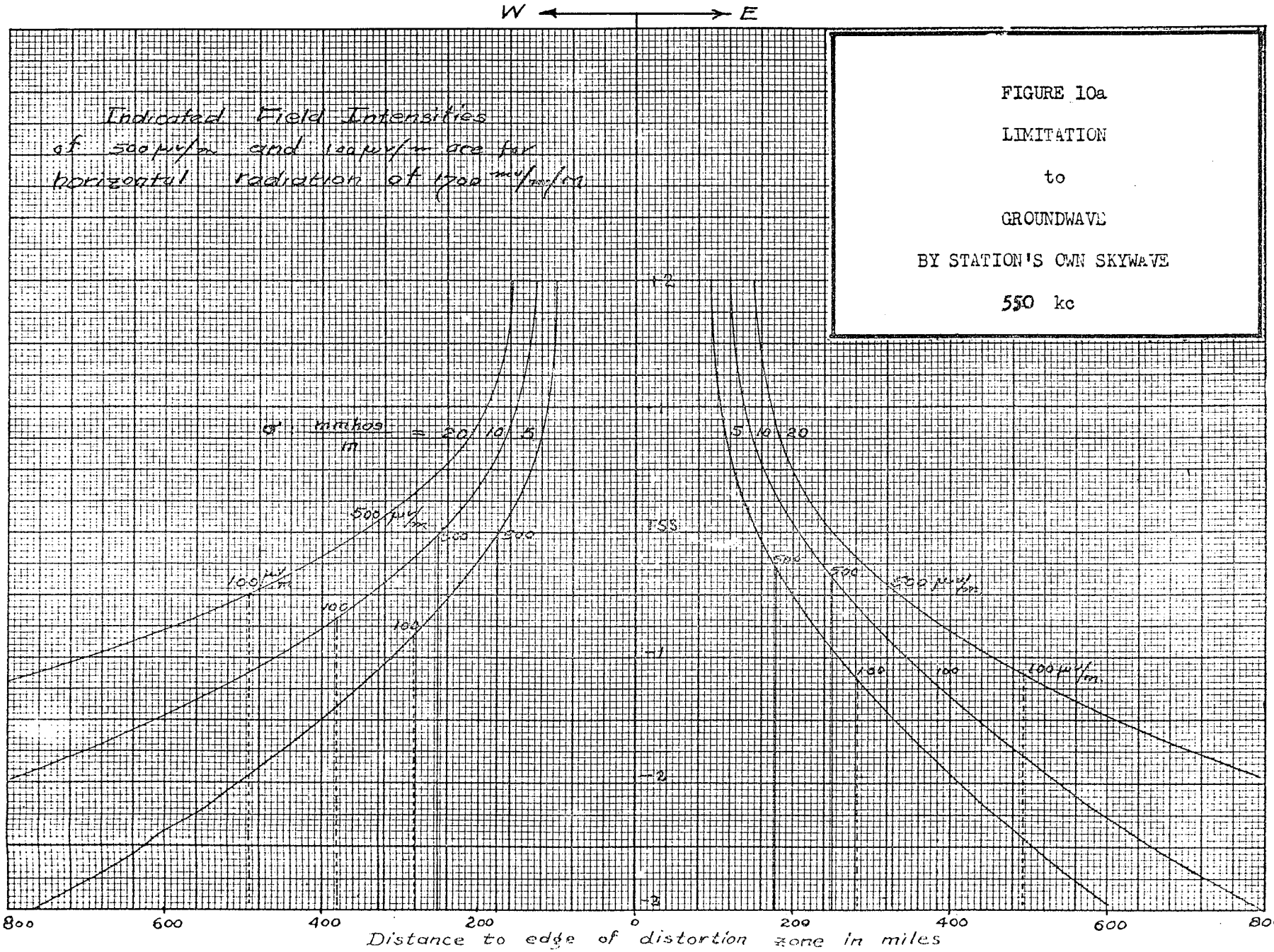

FIGURE 10a

LIMITATION

to

GROUNDWAVE

BY STATION'S OWN SKYWAVE

550 kc

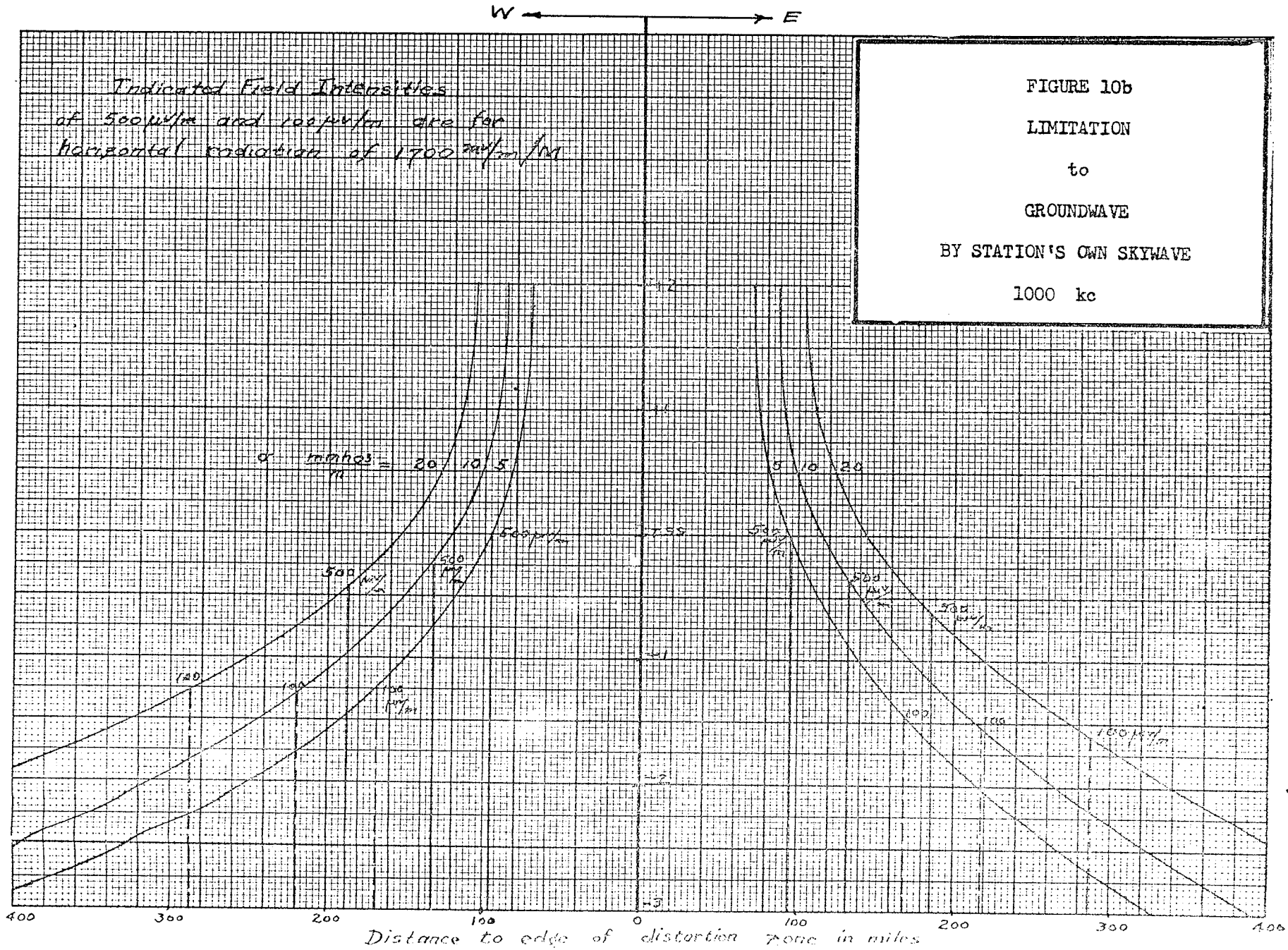
W
E
Indicated Field Intensities of 500 μv/m and 100 μv/m are for horizontal radiation of 1700 mv/m/m
FIGURE 10b
LIMITATION
to
GROUNDWAVE
BY STATION'S OWN SKYWAVE
1000 kc
σ mmho/m = 20 10 5
5 10 20
500 μv/m
100 μv/m
1600 μv/m
400
300
200
100
0
100
200
300
400
Distance to edge of distortion zone in miles

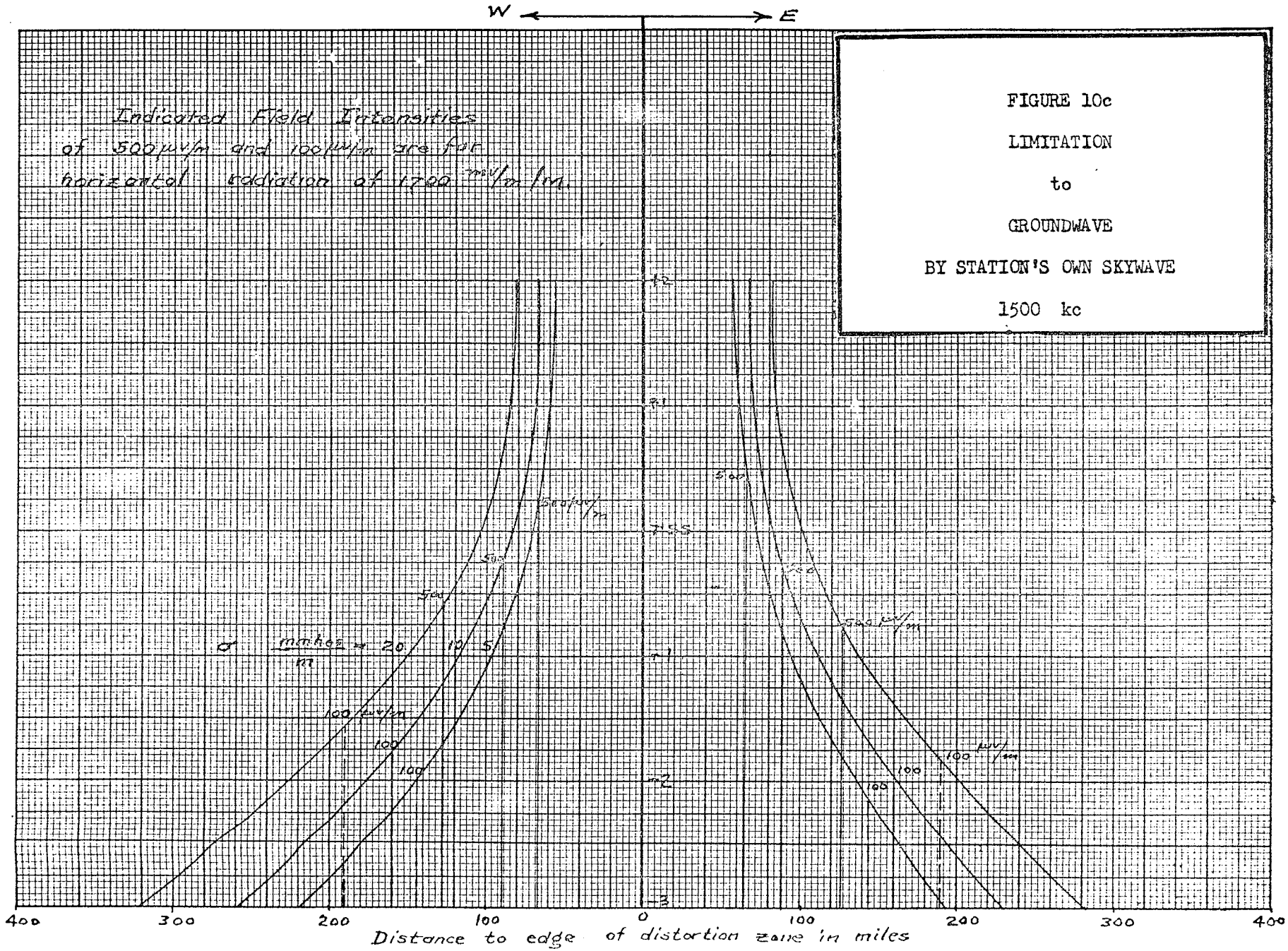
W
E
Indicated Field Intensities of 500 μv/m and 100 μv/m are for horizontal addition of 1700 mv/m fm.
FIGURE 10c
LIMITATION
to
GROUNDWAVE
BY STATION'S OWN SKYWAVE
1500 kc
σ mmhos/m = 20
10
5
500 μv/m
100 μv/m
400
300
200
100
0
100
200
300
400
Distance to edge of distortion zone in miles

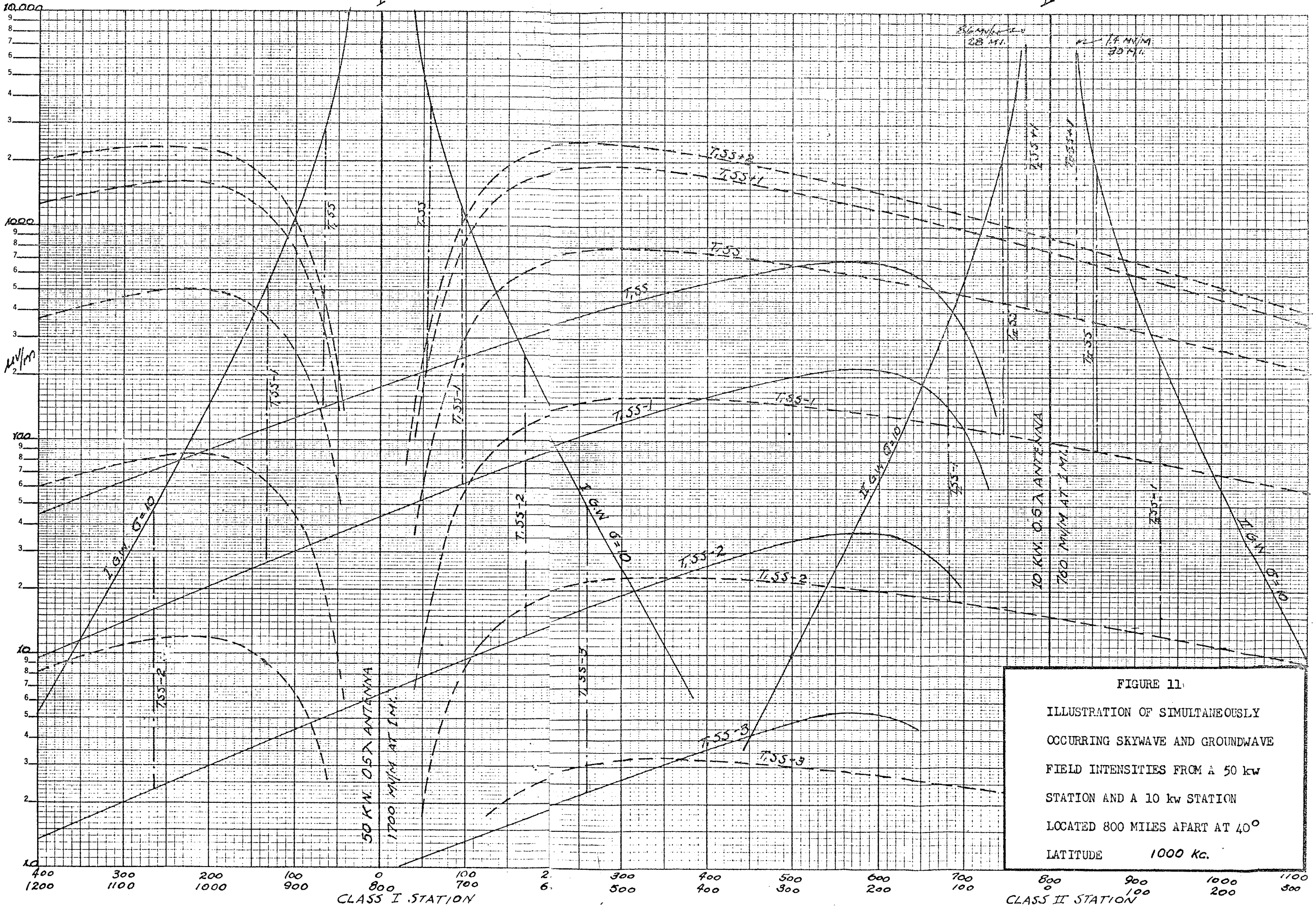

FIGURE 11.

ILLUSTRATION OF SIMULTANEOUSLY OCCURRING SKYWAVE AND GROUNDWAVE FIELD INTENSITIES FROM A 50 kw STATION AND A 10 kw STATION LOCATED 800 MILES APART AT 40° LATITUDE 1000 Kc.

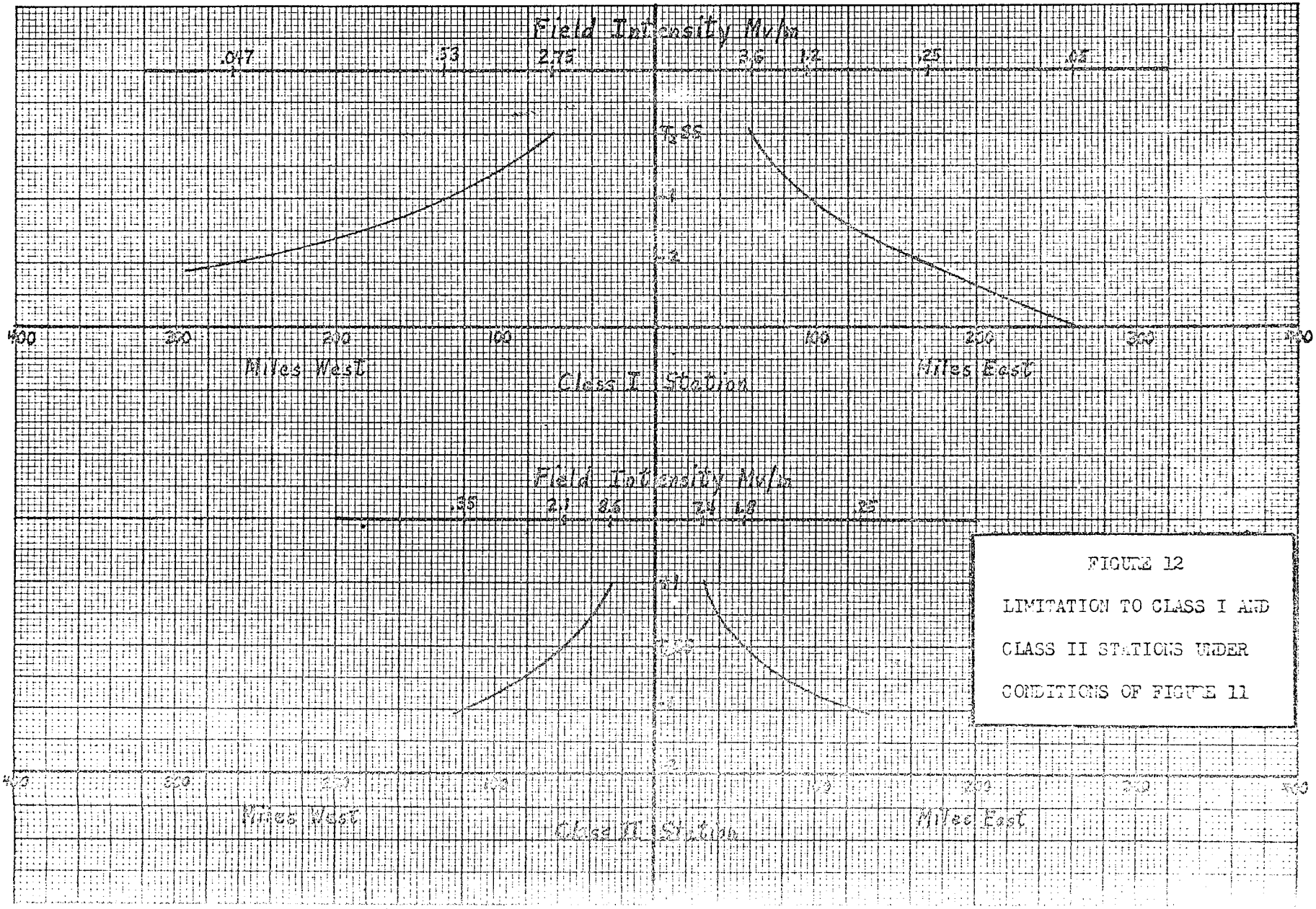

FIGURE 12

LIMITATION TO CLASS I AND CLASS II STATIONS UNDER CONDITIONS OF FIGURE 11